研究简报

配体对功能自组装薄膜的光致电子转移特性的影响

韦天新*,[1] 史环环[1] 黄春辉*,[2] 于小峰[2] 黄慧忠[2] 吴念祖[2]
([1]北京理工大学化学物理研究所,北京 100081)
([2]北京大学稀土材料化学及应用国家重点实验室,北京 100087)

关键词: 薄膜; 表面和界面; 光电转换; 光伏
中图分类号: O641.4 **文献标识码**: A **文章编号**: 1001-4861(2006)06-1077-08

Effects of Connecting Ligands on Photoinduced Electron Transfer Properties of Functionalized Self-assembled Solid Films

WEI Tian-Xin*,[1] SHI Huan-Huan[1] HUANG Chun-Hui*,[2]
YU Xiao-Feng[2] HUANG Hui-Zhong[2] WU Nian-Zu[2]
([1]*Institute for Chemical Physics, Beijing Institute of Technology, Beijing* 100081)
([2]*State Key Laboratory of Rare Earth Materials Chemistry and Applications, PKU, Beijing* 100871)

Abstract: A strategy for fabricating the functionalized self-assembled films is proposed. Through the comparison of three self-assembled films of 3,4,9,10-perylene tetracarboxylic acid (PTA) with different connecting ligands, i.e. oxalic acid (Ox), succinic acid (Su), or terephthalic acid (Tp), it was found that the optimal system was composed of oxalic acid, Ce^{4+} and 3,4,9,10-perylene tetracarboxylic acid,which was much better than simple covalent connecting PTA films and the connecting ligands played an important role for the properties of self-assembled (SA) films. All these films were characterized by contact angle, UV spectra, cyclic voltammetry and XPS. The photocurrent generation of the best system were 5 706, 7 345 $nA \cdot cm^{-2}$, respectively, being among the highest values of dye-sensitized indium tin oxide (ITO) systems. The effects of light intensity, bias voltage, and electron donor on photoinduced electron transfer properties were also studied. The possible mechanism of electron transfer is proposed.

Key words: thin films; surface and interface; photoconductivity; photovoltaics

0 Introduction

The strategy for fabrication of functionalized self-assembled films has been developing rapidly in recent years. Fujihara and his coworkers[1,2] first reported the dehydrative coupling of a carboxyl group of rhodamine B with a surface hydroxyl group to form a presumed ester linkage. Sustained photocurrents from ester-linked tin oxide electrodes were 2 orders of magnitude higher than those obtained from amide-linked silane-pretreated tin oxide surfaces. Soon after, Goodenough et al.[3~5] demonstrated a general method for the attach-

收稿日期:2005-09-12。收修改稿日期:2006-03-16。
国家自然科学基金资助项目(No.20023005,20471009,20573010),教育部留学回国人员科研启动基金,北京理工大学优秀青年教师资助计划(No.000Y07-30)。
*通讯联系人。E-mail:txwei@bit.edu.cn;hch@chemms.chem.pku.edu.cn
第一作者:韦天新,男,36 岁,博士,副教授;研究方向:分子功能膜与器件。

ment of carboxylic acid containing polypyridyl complexes to metal oxides with monolayer surface coverage. Dye-sensitized electron injection is an important basis of color photography[6] and has recently received great attention as the key process in a low-cost, high-efficiency solar cell based on dye-sensitized TiO_2 films[7~9]. Because of the short lifetimes (generally 10^{-8}~10^{-9} s) of the excited states of most metal complexes and organic dyes, they are preferably either absorbed or chemically linked to the surface[10]. Meyer et al.[11] investigated an acetylacetonate-based semiconductor-sensitizer linkage. Now most sensitizers used to dye-sensitized solar cells are connected to electrodes by direct coordination bond or covalent bond with strong adsorbent groups such as carboxyl or hydroxyl phosphonate groups[12]. In addition, at metal oxide interfaces, this chemistry has utilized linkages based on amides[13] and ethers[14].

The self-assembly of dye molecules at the semiconductor oxide surface is a very important strategy to improve the performance of molecular device[15], such as the solar cells. Based on the great achievements of self-assembled (SA) films[16~18] (for excellent reviews see Ref.[19~26]), we report here a new strategy for the sensitization of dyes, by preparing self-assembled films of three complexes layer by layer in situ on indium tin oxide (ITO) substrate.

1 Experimental

1.1 Materials

Dicyclohexylcarbodiimide (DCC) and 1H-benzotriazol-1-ol (BtOH) were purchased from Sigma-Aldrich Co. 3,4,9,10-perylene tetracarboxylic acid (PTA) was prepared by hydrolysis of 3,4,9,10-perylene tetracarboxylic dianhydride (Sigma-Aldrich Co.) following the procedure of E. Keh et al.[27]. Hydroquinone (H_2Q) (Sigma-Aldrich) and all other reagents were AR grade chemicals and used without further purification.

1.2 Fabrication of the films

The fabrication procedure of Film A is shown in Scheme 1. Film A is a monolayer of PTA. It was fabricated as follows: A hydrophilic ITO, or quartz substrates was soaked in a 1 mmol·L^{-1} bromobenzene solution of PTA containing 1 mmol·L^{-1} DCC and 1 mmol·L^{-1} BtOH, and stirred at room temperature for 1~2 days, then rinsed and sonicated in bromobenzene for 2 minutes to remove residual physically adsorbed PTA. The substrate was finally washed by ethanol or acetone and dried in air. The modified surface was confirmed via contact angle, which was changed from

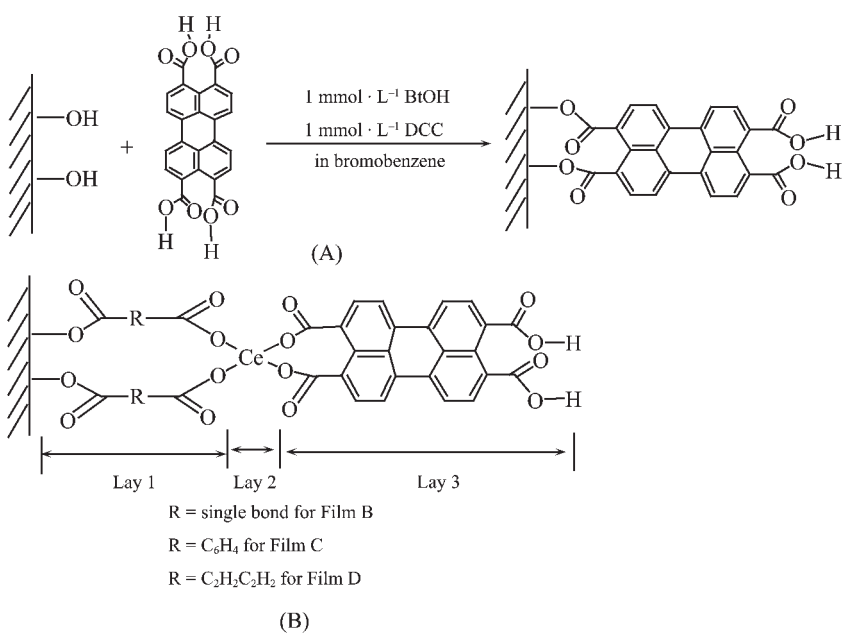

Scheme 1 Synthetic schemes for the formation of Film A (A) and the compositions of Film B to D (B)

20° of the hydrophilic substrate to about 48° of PTA modified substrate. It is not verified whether both carboxyl groups or one of them is bonded to the substrate, but at least one ester bond is formed.

Film B, C and D embody three layers, i.e. connecting ligand, metal ions layer and PTA. For the fabrication of connecting ligands (oxalic acid (Ox), succinic acid (Su), or terephthalic acid (Tp)), self-assembled (SA) film method is similar to that of Film A. After the fabrication of the connecting ligands, the Ox-, Su- or Tp-pretreated ITO was soaked in a 1 mmol·L^{-1} ammonium ceric sulfate (tin tetrachloride, or zirconium oxychloride) of water solution for about half an hour, then rinsed and sonicated in deionized water for 1 min, repeated three times. Finally, the substrate was immersed in 1 mmol·L^{-1} alcohol solution of PTA, then rinsed and sonicated in deionized water for 1 min, repeated three times. The contact angles changed from 20° for hydrophilic substrate to 48°, 39°, 35° or 29° for the Film A to D, respectively (shown in Table 1). The compositions of all these films are shown in Scheme 1.

Table 1　Contact angles, photocurrent generations with and without H_2Q, open circuit voltages (Voc) of Film A to D

SA films	Contact angle[b]	Voc with H_2Q / mV	Photocurrent with H_2Q[a] / (nA·cm^{-2})	Photocurrent without H_2Q[a] / (nA·cm^{-2})
A	48°	104	2 145~3 700	920~1 850
B	39°	139	5 706~7 345	426~733
C	35°	24	1 600~1 692	77~162
D	29°	28	2 050~2 353	280~295

[a] The concentration of H_2Q is 5 mg·mL^{-1}.

[b] The contact angle of hydrophilic ITO is about 20°.

1.3　Instruments and methods

Photoelectrochemical measurements were completed with a three-electrode cell. The film modified ITO electrode, Pt wire and a saturated calomel electrode (SCE) were used as the working electrode, the counter electrode and the reference electrode, respectively. 0.1 mol·L^{-1} KCl solution was used as the electrolyte. The photocurrent measurements and cyclic voltammetry were carried out on a model 600 voltammetric analyzer (CH Instruments Inc., USA) and a 500 W xenon lamp (Ushio Electric, Japan) was used as the light source. A series of filters (Toshiba, Japan) (with the intervals about 50 nm from 400 nm to 800 nm) were used to obtain different wavelengths of incident light. The intensity of incident light was measured by a power and energy meter (Scientech 372, Boulder Co. USA). The IR light was filtered throughout the experiment with a Toshiba IRA-25s filter (Japan) to protect the electrodes from being heated. The UV-Vis absorption spectra were measured by a Shimadzu UV-3100 spectrophotometer. The X-ray photoelectron spectra (XPS) measurement was performed on a VG ESCALAB 5 Multitechnique Electron Spectrometer. The source was Al $K\alpha$ X-rays at 1 486.6 eV with a power level of 180 W. The pass energy was 50 eV. Usually, the accumulative routine was used for spectra acquisition. The base pressure in the sample chamber was 10^{-9} Pa. The binding energy was calibrated by In $3d_{5/2}$.

2　Results and discussion

The films fabricated by the present strategy include three layers (see Scheme 1). So we characterize not only the final full films, but also each layers as much as possible.

2.1　Characterization of the layer 1 of Film B, C and D

The contact angles of the Ox-pretreated, Su-pretreated and Tp-pretreated ITO are changed from 20° of hydrophilic ITO surface to 34°, 41° and 39°, respectively. Besides the contact angles, the Ox, Tp and Su pretreated ITOs are also characterized by their cyclic voltammetries (CVs). Fig.1 shows the cyclic voltammetries of the Ox-, Su- and Tp-pretreated ITOs. The Ox-pretreated ITO is the largest among the three acids shown in Fig.1. This is another evidence of the successful modifications of layer 1.

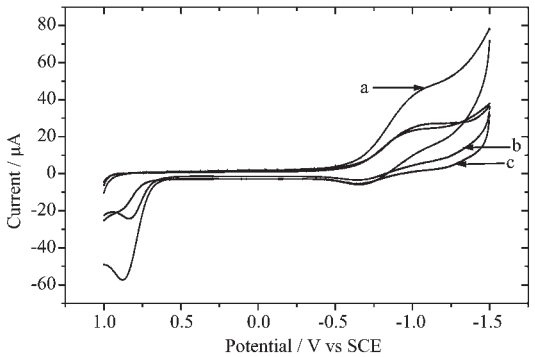

Fig.1 Cyclic voltammetries of Ox-pretreated ITO (a), Su-pretreated ITO (b) and Tp-pretreated ITO (c)

2.2 Characterization of the layer 2 of Film B, C and D

2.2.1 X-ray photoelectron spectroscopy

Ce3$d_{5/2}$ (881.8 eV) and Ce3$d_{3/2}$ (900.1 eV) are all observable in the XPS of Film B, C and D on ITO in the region of 875~925 eV binding energy as shown in Fig.2. The signals of metal ion Ce^{4+} are the direct evidence for our proposed structures of these films (shown in Scheme 1).

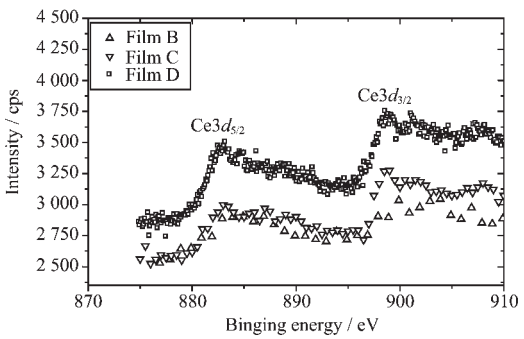

The detector is 0° off the surface normal

Fig.2 XPS spectra of Film B, C and D on ITO electrode

2.3 Characterization of Film A and full Film B, C and D

2.3.1 Absorption spectra

The UV-Vis absorption spectra of Film A and B on quartz are shown in Fig.3 (A). Three absorption peaks at 231, 285 and 330 nm are observed for Film A and three peaks at 217, 301 and 483 nm are seen for Film B, while the peaks of PTA in ethanol solution are at 226 nm and 302 nm. The peak at 483 nm of Film B is assigned to the ligand metal charge transfer (LMCT) absorption of the ligand PTA to central metal Ce^{4+}. The UV-Vis absorption spectra of Film C and D on ITO are shown in Fig.3(B). All these Ce^{4+} containing films have a new absorption peak at 483 nm in the visible region, implying that this peak is related to the LMCT absorption of PTA and Ce^{4+}. The data show that Ce^{4+} improves the absorption property of the films significantly by the LMCT absorption.

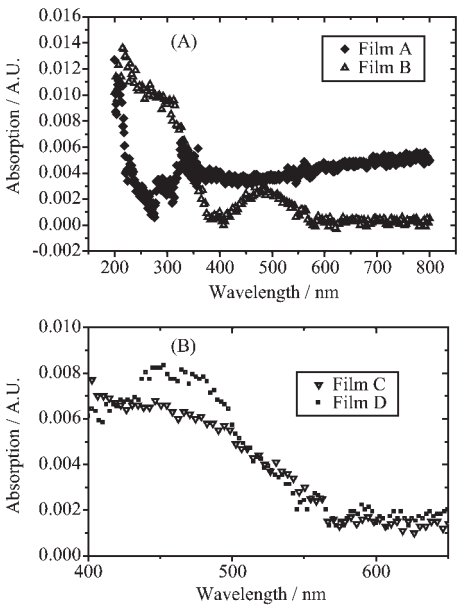

Fig.3 Absorption spectra (A) Film A and B on quartz (B) Film C and D on ITO

2.3.2 Electrochemical properties

The CVs of Film A and B are shown in Fig.4 (A) and (B) for comparison. The Film B is composed of Ox, Ce^{4+} and PTA, its CV reveals two reduction peaks at −0.20 V and −0.87 V, and two oxidation peaks at 0.16 V and −0.41 V. The large difference between the anodic current (0.5×10^{-4} A) and the cathodic current (1.1×10^{-4} A) implies that there may be an irreversible chemical reaction on the electrode.

The difference (ΔE) between the oxidation and reduction potentials of Film B (1.03 V) is much smaller than that (2.1 V) of Film A, indicating that the kinetic process in Film B system is faster than that in Film A[28]. Metal ion Ce^{4+} accelerates the electrochemistry process of PTA in Film B by its bridging role.

2.4 Photoelectric properties of all films

2.4.1 Photoelectric response

The photocurrent generated with and without H_2Q and open circuit voltage (Voc) of the Film A to D are shown in Table 1. All systems generate stable anodic

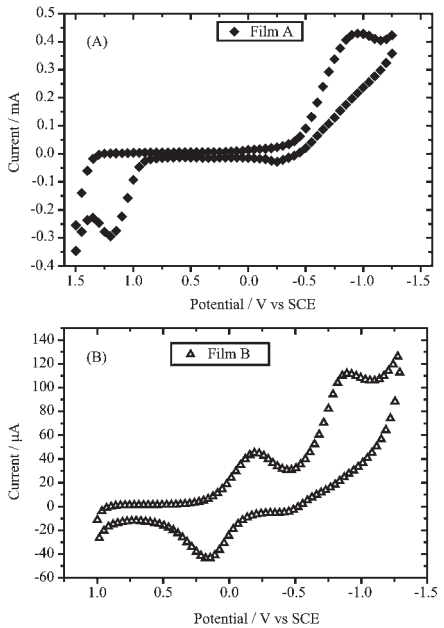

Conditions: the working electrode: ITO, the counter electrode: a platinum wire and the reference electrode: a saturated calomel electrode (SCE)

Fig.4　Cyclic voltammetries of Film A (A) and Film B (B) in water solution containing 0.1 mol·L^{-1} Bu_4NClO_4

photocurrent. The results of Film B, C and D indicate that oxalic acid is the best connecting ligand. The largest photocurrent generation of 5 706~7 345 nA·cm^{-2} is produced by the Film B after addition of 5 mg·mL^{-1} H_2Q, while the hydrophilic-pretreated ITO substrate can generate the anodic photocurrent only 7 nA·cm^{-2}. The value of the photocurrent generation of Film B is one of the largest values of dye-sensitized ITO systems[29]. For all parameters, the order is Film B > Film D > Film C. The photocurrent generation of Film B is 2 times larger than that of Film D and 3 times of Film C. The open circuit voltage of Film B even improves more and is about 5 times of Film D and C. The data show that the connecting ligands are very important for the photoinduced electron transfer properties of this kind of SA films.

In order to understand these results, we calculated three connecting ligands by AM1 in CHEM 3D, one software in CS ChemOffice. The distances between two carbon atoms in two dicarboxylic acid group of each molecule are 0.149, 0.381 and 0.575 nm for Ox, Su and Tp molecule, respectively. The distance order just coincides with the order of photoinduced electron transfer of the titled SA films, indicating that electrons may transfer across the connecting ligand through tunneling effect. So the processes are mainly related to the length of molecules and not related to the conjugations and energies of molecular orbital.

2.4.2　Action spectra

The action spectrum of the photocurrent generation of the Film B and its UV-Vis spectrum are shown in Fig.5 (A). The intensities for different wavelengths are all normalized. The action spectrum was recorded under the irradiation of different wavelengths from a white light (200 mW·cm^{-2}). The shape of the action spectrum coincides well with the curve of its UV absorption spectrum, indicating that the Ox-Ce^{4+}-PTA trinary complex in the film is responsible for the photocurrent generation. At the wavelength of 497 nm, the quantum yield of this system is 2.3%, suggesting that it is one of the most efficient dye-sensitized ITO

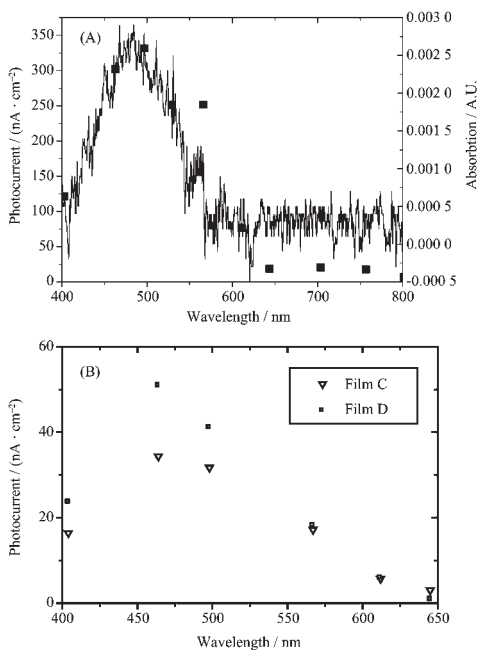

The concentration of the electrolyte solution is 0.1 mol·L^{-1} KCl. The intensities for different wavelengths are all normalized.

Fig.5　Action spectrum (■) and the UV-Visible absorption spectrum (—) of Film B (A) and the action spectra of Film C and Film D (B) on the hydrophilic ITO under irradiation of white light at 200 mW·cm^{-2} with bias potential of 100 mV

systems, as far as we know. The action spectrum of Film A was too weak to be determined. The action spectra of Film C and D are shown in Fig.5(B). These curves are also coincides well with the curves of their corresponding UV absorption spectra (shown in Fig.2 (B)). The results confirm the successful fabrication of these SA films.

2.5 Effect of light intensity, electron donor and bias voltage

The relationship between the photocurrent generation of Film A to D and the light intensity is shown in Fig.6. According to Donoan[30] theory, in the titled systems, the separated charge loss is through monomolecule recombination. When the electron donor (H_2Q) is added to the electrolyte solution, an increase of the photocurrent generation from each film can be observed (shown in Fig.7). The hydroquinone donates electrons to the trinary complex on the surface of ITO electrode to maintain the concentration of photoelectric active substance and increases the concentration of electrons in the electron transition. This improves the electron transfer and increases the photocurrent subsequently. Data show that the increase in photocurrent of Film B is much larger than that of Film A, C and D. This phenomenon indicates the charge separation or charge injection rates in the system of Film B may be faster than those in the rest systems. The photocurrent of Film A to D increases with the increase of the positive bias potential, and decreases with the increase of the negative bias potential added to the working electrode as shown in Fig.8. This fact indicates that the electron is transferred from the electrolyte through the film to ITO. The increase of photocurrent for Film B is more sensitive to bias potentials than the rest films, implying that the effect of charge separation for Film B is much larger. The open circuit voltage (Voc) can be obtained by extension of the photocurrent-voltage linear line. The Vocs of these systems are shown in Table 1. The largest Voc of 139 mV for Film B implies that its energy level of the lowest unoccupied molecular orbital (LUMO) may be the highest among the three trinary complexes in the SA films.

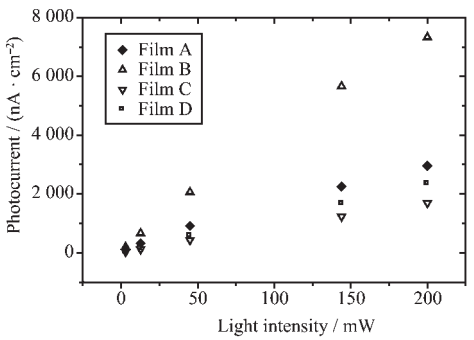

The concentration of the electrolyte solution is 0.1 mol·L^{-1} KCl. The effective irradiation area is 1.5 cm^2.

Fig.6 Relationships between photocurrent generation of Film A to D and light intensities without bias potentials

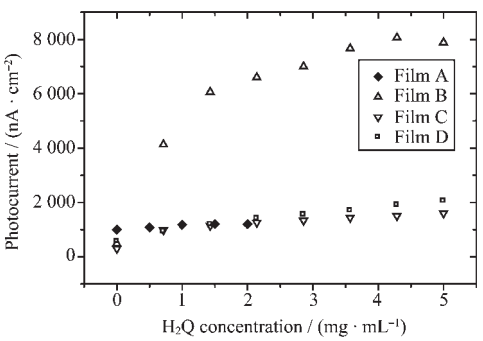

Fig.7 Effects of the concentration of electron donor H_2Q on the photocurrent generation of Film A to D at the electrolyte concentration of 0.1 mol·L^{-1} KCl and the effective irradiation area of 1.5 cm^2

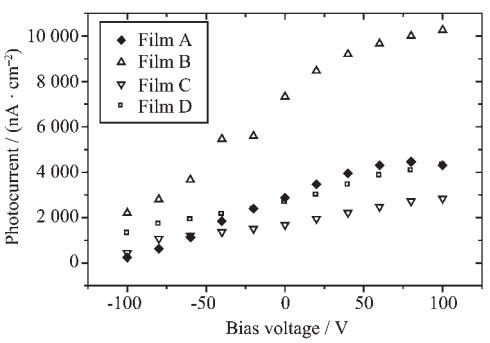

Fig.8 Effects of bias voltage on the photocurrent generation of Film A to D at the electrolyte concentration of 0.1 mol·L^{-1} KCl and the effective irradiation area of 1.5 cm^2

2.6 Possible mechanisms

Film A and Film B are selected as the examples for two kinds of films. Scheme 2 shows the possible mechanisms of the photocurrent generation of the systems for Film A (A) and Film B (B). The electron

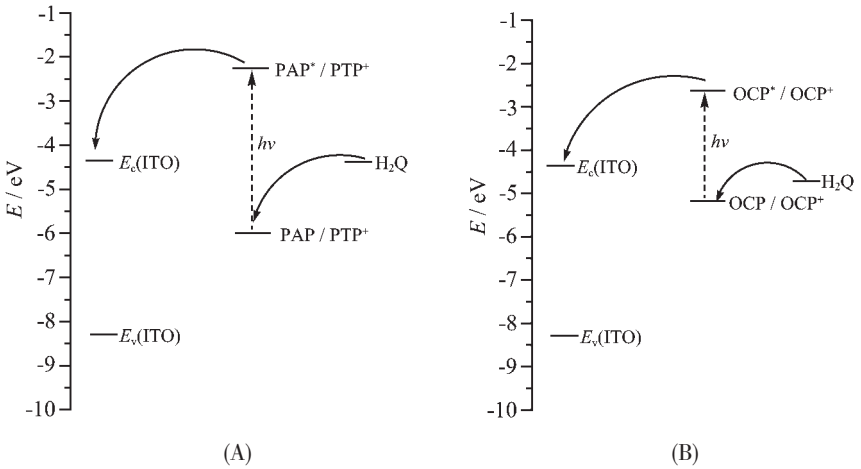

PTA and OCP represent the ground state of PTA and Ox-Ce^{4+}-PTA trinary complex

PTA^* and OCP^* represent their excited states, PTA^+ and OCP^+ stand for their oxidized states

Scheme 2　Possible mechanisms of photoindued electron transfer systems of Film A (A) and Film B (B)

affinity of the conduction band (E_c) and valence band (E_v) of the ITO electrode are estimated to be −4.5 and −8.3 eV [31], respectively. The oxidation potential of H_2Q is −4.61 eV (0.23 V vs SCE) on an absolute scale[32]. From the results of cyclic voltammetry and the UV-Vis spectrum of Film B the oxidation energy level of PTA is about −4.9 eV (0.16 V vs SCE), the oxidation energy level of Ce^{4+} is about −4.54 eV (−0.2 V vs SCE) and the excited reduction energy level of PTA is assumed to be about −2.34 eV (the band gap between them is 483 nm on ITO electrode, which equals to 2.56 eV). From the results of cyclic voltammetry and the UV-Vis spectrum of Film A, the oxidation energy level of PTA is about −6.0 eV (1.26 V vs SCE), and the excited reduction energy level of PTA is assumed to be about −2.25 eV (the band gap between them is 330 nm on ITO electrode, which equals to 3.75 eV).

For the system of Film A, as shown in Scheme 2 (A), when the light irradiates on the electrode, PTA is excited from its ground state to its excited state to form PTA^*. Then PTA^* gives out electron to the conduction band of ITO and becomes oxidized as PTA^+. PTA^+ accepts electron from electron donor H_2Q in the electrolyte and completes the circuit.

For the system of Film B, the mechanism is shown in Scheme 2 (B). When the light excites the complex of Ox-Ce^{4+}-PTA (OCP) from its ground state to its excited state to form OCP^*, then the OCP^* gives out electron to the conduction band of ITO to become OCP^+. Then OCP^+ accepts electron from electron donor H_2Q in the electrolyte and completes the circuit.

3　Conclusions

Through a new strategy, three functionalized self-assembled films were successfully fabricated. The photoinduced electron transfer property of the optimal system of Film B fabricated by self-assembly technology is much better than that of the system of Film A fabricated by the conventional method. The choice of the connecting ligands is one of the important factors for the properties of the SA films.

References:

[1] Fujihira M, Ohishi N, Osa T. *Nature*, **1977**,**268**:226~228

[2] Fujihara M, Kubota M, Osa T. *J. Electronal. Chem.*, **1981**, **119**:379~387

[3] Anderson S, Constable E C, Goodenough J B. *Nature*, **1979**, **280**:571~573

[4] Goodenough J B, Hamenett A, Dare-edwards M P. *Surf. Sci.*, **1980**,**101**:531~540

[5] Dare-edwards M P, Goodenough J B, Hamenett A, et al. *Faraday Discuss. Chem. Soc.*, **1980**,**70**:285~298

[6] Carroll B H. *Introduction to Photographic Theory*. New York: Wiley, **1980**.

[7] O′Rengan B, Graetzel M. *Nature*, **1991**,**353**:737~740

[8] Nazeeruddin M K, Kay A, Graetzel M, et al. *J. Am. Chem.*

Soc., **1993**,**115**:6382~6390

[9] Heimer T S, Bignozzi C A, Meyer G J. *J. Phys. Chem.*, **1993**, **97**:11987~11994

[10]Kalyanasundaram K, Graetzel M. *Photosensitization and Photocatalysis Using Inorganic and Organometallic Compounds*, Netherlands, Kluwer Academic Publishers, **1993**:248

[11]Heimer T A, D′Arcangelis S T, Meyer G J, et al. *Inorg. Chem.*, **1996**,**35**:5319~5324

[12]Pechy P, Rotzinger F P, Graetzel M. *J. Chem. Soc., Chem. Commun.*, **1995**:65

[13]Moses P R, Murray R W. *J. Electroanal. Chem.*, **1977**,**77**: 383~386

[14]Zou C, Wrighton M S. *J. Am. Chem. Soc.*, **1990**,**112**(21):7578~7584

[15]Swalen J D, Allara D L, Andrade J D, et al. *Langmuir*, **1987**,**3** (6):932~950

[16]Jeon N L, Nuzzo R G. *Langmuir*, **1995**,**11**(8):3024~3026

[17]Sagiv J. *J. Am. Chem. Soc.*, **1980**,**102**(1):92~98

[18]Wasserman S R, Whitesides G M, Tidswell I M, et al. *J. Am. Chem. Soc.*, **1989**,**111**(15):5852~5861

[19]Ulman A. *Chem. Rev.*, **1996**,**96**(4):1533~1554

[20]Xia Y N, Rogers J A, Paul K E, et al. *Chem. Rev.*, **1999**,**99**: 1823~1848

[21]Fendler J H, Meldrum F C. *Adv. Mater.*, **1995**,**7**:607~610

[22]Li D Q, Smith D C, Hawley M E, et al. *Chem. Mater.*, **1992**, **4**(5):1047~1053

[23]Evans S D, Ulman A, Gerenser L J, et al. *J. Am. Chem. Soc.*, **1991**,**113**(15):5856~5857

[24]Bell C M, Arendt M F, Mallouk T E, et al. *J. Am. Chem. Soc.*, **1994**,**116**(18):8374~8375

[25]Ansell M A, Zeppenfeld A C, Page C, et al. *J. Chem. Mater.*, **1996**,**8**:591~594

[26]Lee H, Kepley L J, Mallouk T E, et al. *J. Am. Chem. Soc.*, **1988**,**110**(2):618~620

[27]Keh E, Valeur B. *Journal of Colloid and Interface Science*, **1981**,**79**:465~478

[28]Imahori H, Norieda H, Sakata Y, et al. *Langmuir*, **1998**,**14** (19):5335~5338

[29]Zheng J, Wu D G, Zhai J, Gao X C, et al. *Phys. Chem. Chem. Phys.*, **1999**,**1**:2345~2349

[30]Donoan K J, Sudiwala R V, Wilson E G. *Mol. Cryst. Liq. Cryst.*, **1991**,**194**:337~342

[31]Sereno L, Silber J J, Gust D, et al. *J. Phys. Chem.*, **1996**, **100**(2):814~821

[32]Kim Y S, Liang K, Whitten D G, et al. *J. Phys. Chem.*, **1994**, **98**(3):984~988